Electronic Supplemental Information

Part 1 – Angular cross-correlation

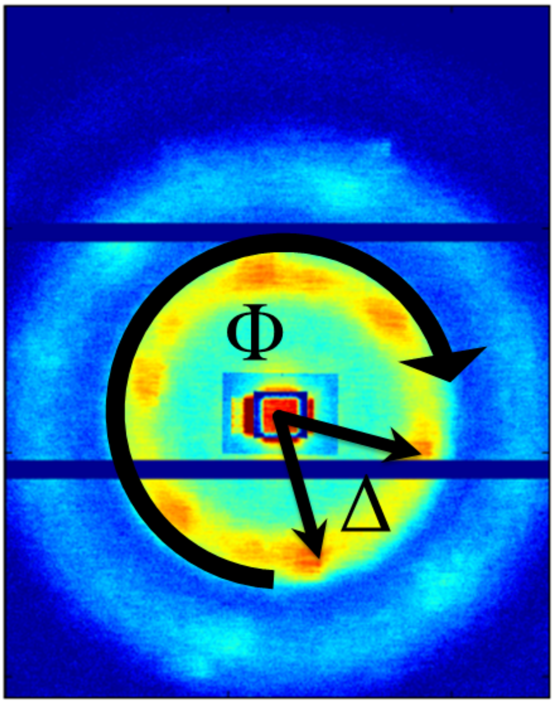

SI-1: Definition of the angular cross-correlation. Φ denotes the azimuthal angle and Δ the angle between two points on a scattering intensity annulus.

Fig. SI-1 shows a typical two-dimensional scattering pattern. The definition of the angular cross-correlation function for such a pattern at fixed wave vector transfer *Q* is [1,2]:

$$C(Q,\Delta) = \frac{\langle I(Q,\Phi) I(Q,\Phi+\Delta)\rangle_\Phi - \langle I(Q,\Phi)\rangle_\Phi^2}{\langle I(Q,\Phi)\rangle_\Phi^2}. \quad (SI1)$$

Herein, Δ denotes the angle between two points on an intensity annulus *I*(*Q*) with radius *Q*. For these the cross-correlation is computed by taking the product of all points at given angle Φ on the annulus that are separated by Δ. $\langle \cdot \rangle_\Phi$ denotes the angular average over such an annulus.

Part 2 – Superlattice structures AB_2 and AB_{13}

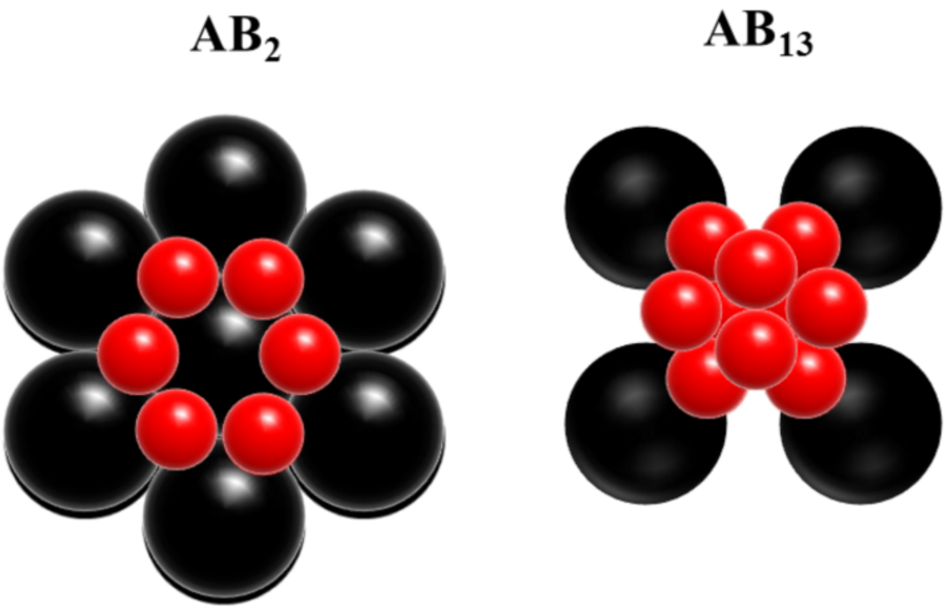

SI-2 – AB_2 structure and AB_{13} structure.

Binary mixtures of colloids can form crystals with superlattice structures. Common superlattice structures are the AB_2 and AB_{13} structures (Fig. SI-2). 'A' denotes the large particle species, 'B' the small one.

The hexagonal AB_2 structure consists of a hexagonal closed packing of large particles. The small particles form planar rings filling the holes between the larger particles [3].

In the AB_{13} structure, the large particles form a simple cubic structure. Within this cube, a body-centered small particle is located which is surrounded by 12 other small particles in an icosahedral structure [3].

The stability of these superlattices depends on the radius ratio α. For $0.425 < \alpha < 0.60$, the AB_2 structure is stable, and for $0.485 < \alpha < 0.62$, the AB_{13} structure is stable [4]. As the radius ratio of the silica particles used was $\alpha = 0.58$, both structure are expected to be present within the colloidal film.

Part 3 – Results of a binary colloid film with *X* = 0.89

In the following the scanning SAXS and XCCM results on a dried colloidal film with particle size ratio α = 0.58 and mixing ratio *X* = 0.89 are presented. The experimental conditions were the same as described in the main part.

Part 3.1 – Intensity maps for *X* = 0.89

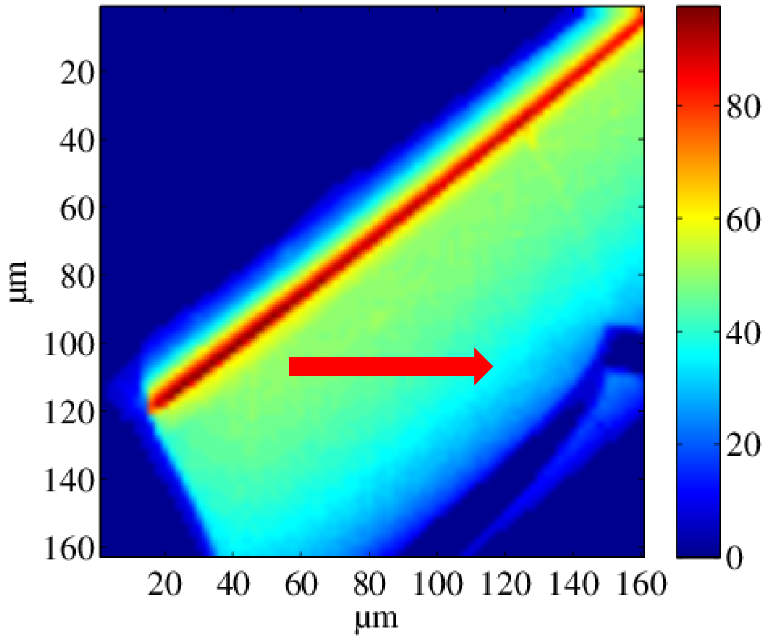

SI-3 – Intensity map for X= 0.89, Q_1.

Fig. SI-3 shows the scanning map of the scattering intensity of the Q_1 – partition. Clearly visible are the sharp edges of the dried colloidal film. The strongest scattering intensity is detected for a pronounced stripe in the upper part close to the edge of the film. In contrast, for the region below a continuous reduction of the scattering intensity is present.This points towards a particle density gradient in the film (indicated by the red arrow).

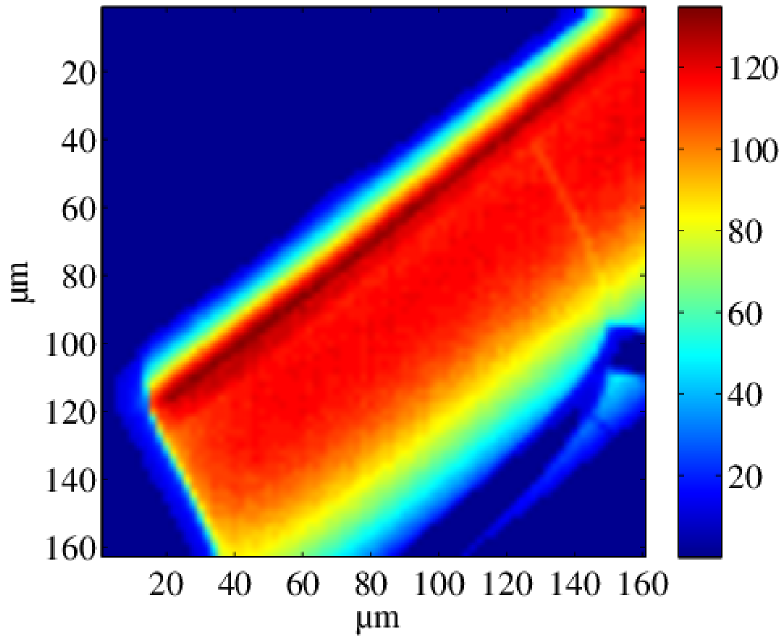

SI-4 – Intensity map for X= 0.89, Q_2.

Compared to the Q_1 - partition, the scattering intensity of the Q_2 – partition (Fig. SI-4) is in general stronger because the small particle species is dominating within the sample. In contrast to the intensity map at Q_1, the intensity gradient is weaker in the film. This suggests that the large silica particles are mainly contained in the stripe-like region close to the upper film edge. The small particles are distributed everywhere in the film. Thus, for this sample particle segregation within the drying process took place.

Part 3.2 – Cross-correlation maps for $X = 0.89$

Figures SI-5 to SI-10 display the XCCM maps for $l = 2$, 4 and 6 for both Q-partitions. As for the $X = 0.66$ sample, a strong $l = 2$ contribution is present at the film edge at Q_1. For the other parts of this film, the $l = 4$ contribution is stronger than the $l = 2$ contribution. The region where the large particle species is more dominantly present, i.e. the stripe region, has a reduced four-fold order compared to the other parts of the sample. Notable is one ordered region containing only the large particles (Fig. SI-5 to SI-7 in the upper right corner).

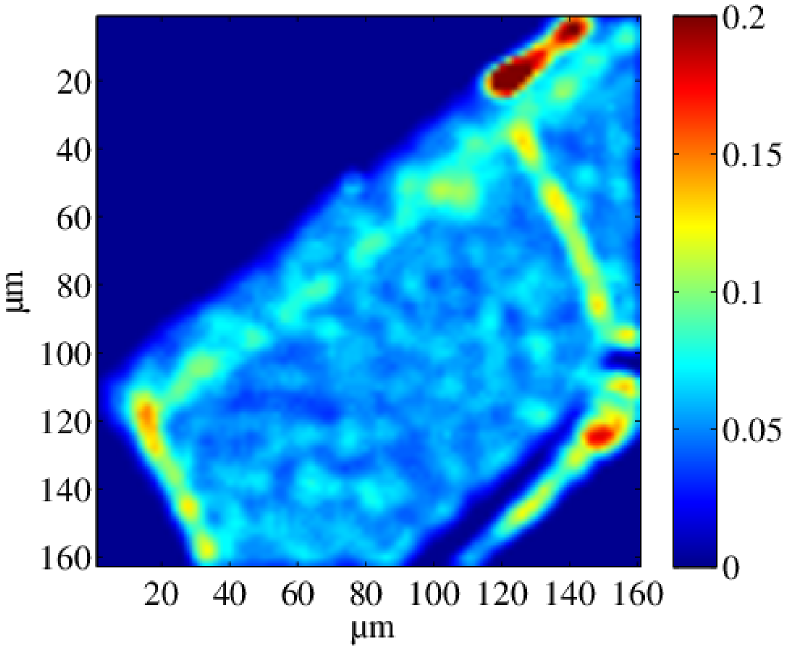

SI-5 – XCCM map Q_1, $l = 2$.

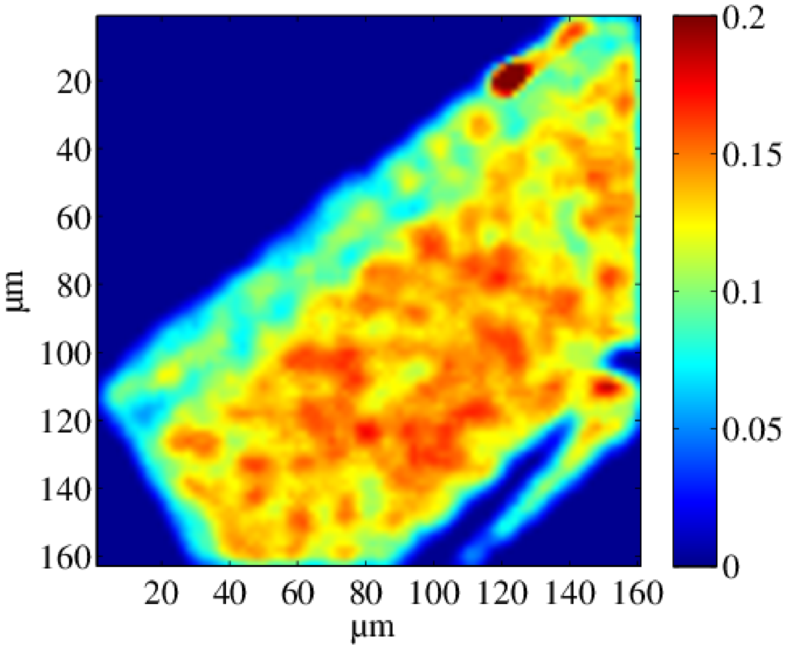

SI-6 – XCCM map Q_1, $l = 4$.

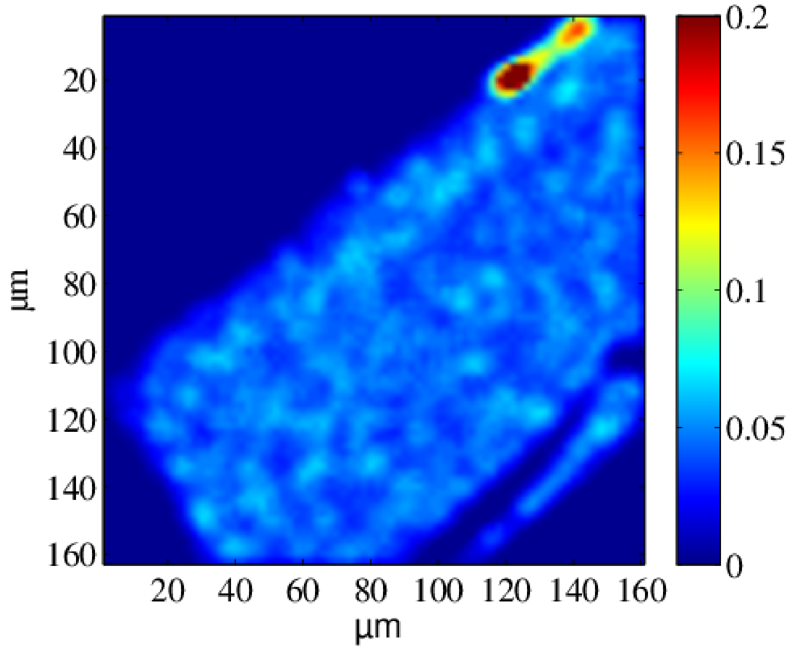

SI-7 – XCCM map Q_1, l = 6.

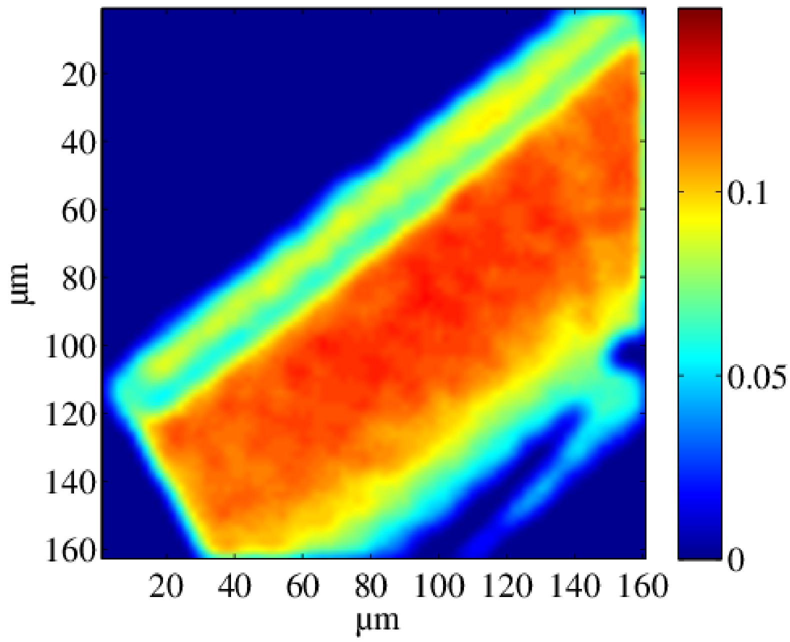

SI-8 – XCCM map Q_2, l = 2.

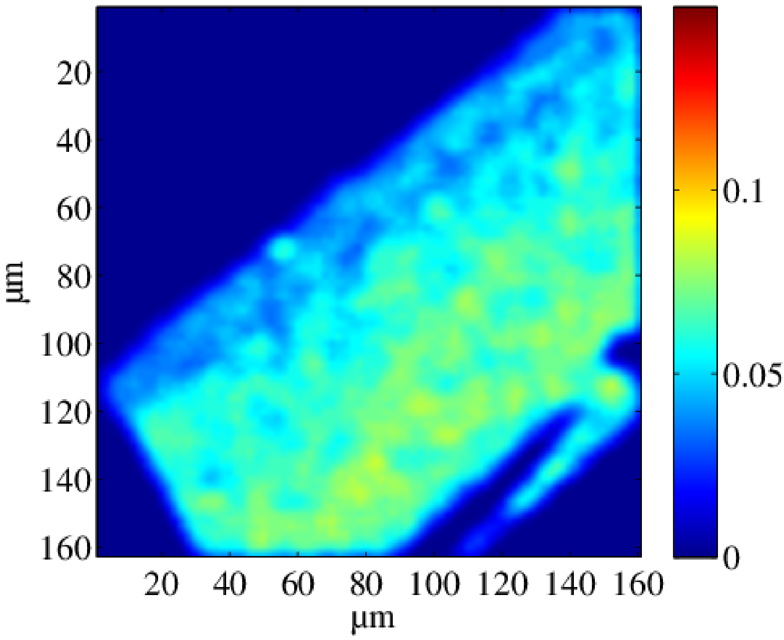

SI-9 – XCCM map Q_2, l = 4.

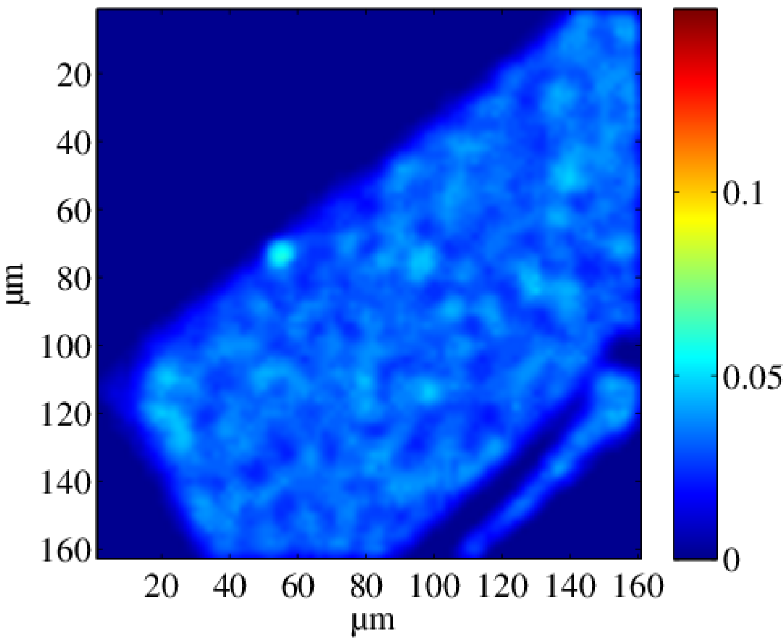

SI-10 – XCCM map Q_2, l = 6.

Part 3.3 – Map sections for X = 0.89

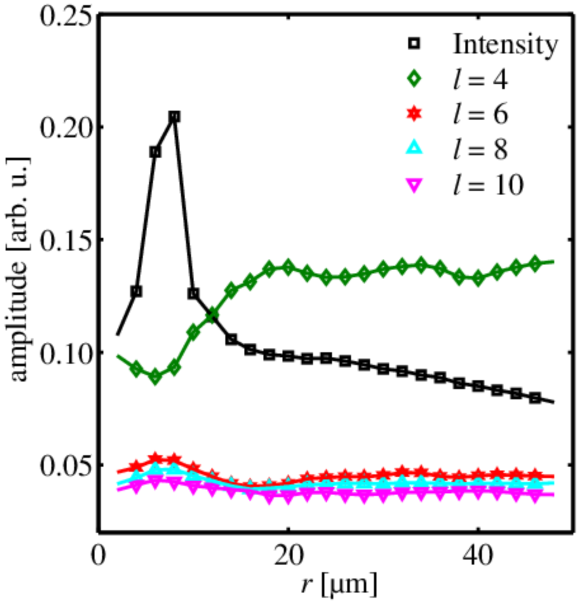

SI-11 – Map section for Q_1.The l = 2 component, being only an indicator for the film edges, is not shown.

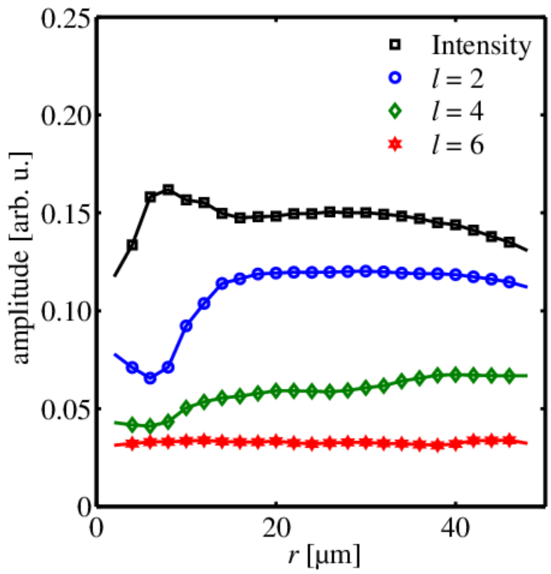

SI-12 – Map section for Q_2.

Fig. SI-11 and SI-12 show the results of the sections of the intensity and XCCM maps for both Q-partitions along the red arrow (see Fig. SI-3) averaging along the full film size. For Q_1 the prounced stripe as well as the decreasing particle density are visbile from the intensity curve. In case of the cut for the Q_2 map, the scattering intensity is neither that strong at the stripe region nor is the particle gradient that strong indicating a more homogenous distribution of small particles.

For the Q_1-partition the $l = 4$ contribution is the most dominant Fourier component. It is reduced in the stripe-region indicating a reduced order due to the high fraction of large silica particles. The $l = 4$ curve is nearly constant along the other part of the film for Q_1. The other Fourier components studied, i.e. $l = 6$-10, have reduced amplitudes of similar values and show small maxima at both the stripe region and within the small particle region.

In contrast, for the Q_2 map the $l = 2$ Fourier component is the strongest component. It exhibits a minimum in the stripe region and is nearly constant within the other part of the film. The $l = 4$ component has a smaller amplitude but a similar shape. The $l = 6$ component is nearly constant. This finding is similar to that for the film with $X = 0.66$.

References

[1] P.Wochner, C. Gutt, T. Autenrieth, T. Demmer, V. Bugaev, A. D. Ortiz, A. Duri, F. Zontone, G. Grübel, and H. Dosch, *Proc. Natl. Acad. USA* **106**, 11511 (2009).

[2] M. Altarelli, R. P. Kurta, and I. A. Vartanyants, *Phys. Rev. B* **82**, 10 (2010).

[3] M.J. Murray and J.V. Sanders, *Philos. Mag. A* **42**, 721 (1980).

[4] A.B. Schofield, P.N. Pusey, and P. Radcliffe, *Phys. Rev. E* **72**, 031407 (2005).